Hindawi
Shock and Vibration
Volume 2020, Article ID 2128045, 13 pages
https://doi.org/10.1155/2020/2128045

Research Article

Experimental Study on Characteristics of Seismic Damage and Damping Technology of Absorbing Joint of Tunnel Crossing Interface of Soft and Hard Rock

Dao-yuan Wang,[1,2] Jin-xiu Yuan ,[1] Guang-yao Cui,[3] Jia Liu,[1] and Hong-fan Wang[2]

[1]*Department of Civil Engineering, Hebei Jiaotong Vocational and Technical College, Shijiazhuang, Hebei 050091, China*
[2]*School of Civil Engineering, Shijiazhuang Tiedao University, Shijiazhuang, Hebei 050043, China*
[3]*School of Civil Engineering, North China University of Technology, Beijing 100144, China*

Correspondence should be addressed to Jin-xiu Yuan; xiugirl2007@163.com

Received 9 February 2020; Revised 16 June 2020; Accepted 3 July 2020; Published 24 July 2020

Academic Editor: Piotr Folęga

It has generally been believed that the serious seismic damage of tunnel mainly occurred in portal section and fault dislocation zone. However, the survey of seismic damage showed that the seismic damage of tunnel also mainly occurred in geological section at interface of soft and hard rock. Currently, merely scholars have made some research studies on characteristics of seismic damage and damping technology of tunnel crossing the vertical interface between soft and hard rock in high intensity area, and the mechanism of seismic damage has not been clearly revealed. Therefore, based on the Urumqi Metro Tunnel project in China, a three-dimensional six-degree-of-freedom shaking table model test was carried out. Through comparative analysis of peak ground acceleration (PGA), displacement difference at the interface between soft and hard rock, and structural safety factor under 5 kinds of conditions, the seismic damage characteristics of tunnel crossing interface of soft and hard rock were revealed, and a new damping technology of absorbing joint was proposed. The following findings can be drawn. (1) The seismic damage of tunnel is mainly affected by stratum inertial force under the homogeneous stratum of soft rock. The seismic damage of tunnel is mainly caused by the forced displacement (the displacement difference between the two sides of interface of soft and hard rock), followed by stratum inertial force under the geological condition of interface between soft and hard rock. (2) The conventional type of absorbing joint (only the second lining is set with absorbing joint) is used in tunnel lining structure, and the damping ratios of principal tensile stress, bending moment, and axial force of lining are above 47.5%, 40.7%, and 72.7%, respectively. Compared with conventional type of absorbing joint, the damping effect of new type of absorbing joint (staggered absorbing joints of primary support and secondary lining) is 19.9% higher than that of conventional type. (3) The new type of absorbing joint is recommended for tunnel crossing interface section of soft and hard rock. The specific implementation suggestions are as follows: the setting interval of second lining absorbing joint is the same as the length of lining formwork trolley, and the interval of primary support absorbing joint can be set according to excavation footage length. The filling materials in second lining absorbing joint can be shared with the rubber waterstop set in construction joint, and the primary support absorbing joint can be realized by injecting mixtures of rubber particles and shotcrete.

1. Introduction

The seismic performance of tunnel mainly depends on the geological conditions to a certain extent; the portal section and fault dislocation zone of tunnel are generally the most severely sections of seismic damage. Many scholars have conducted research on antiseismic mechanism, measures, and antiseismic fortification length of tunnel by using methods of seismic damage investigation, theoretical analysis, numerical calculation, and model test for severe seismic damage sections mentioned above, and a large number of relevant research results have been achieved [1–6]. However,

the survey of seismic damage after Wenchuan earthquake in China showed that the seismic damage of tunnel also mainly occurred in geological section at interface of soft and hard rock, and the tunnel linings were peeled, cracked, staggered, and collapsed in different degrees, such as the Baiyunding Tunnel from the G213 highway of Yingxiu to Dujiangyan in Sichuan Province and Longxi Tunnel on the Yingdu expressway. The tunnel linings of interface section between soft and hard rock on these two lines showed circumferential cracks with 1 cm~3 cm widths after earthquake [2, 7–15].

Currently, merely scholars have made some research studies on antiseismic technology of tunnel passing through interface of soft and hard rock. Over 30 tunnels after the Wenchuan earthquake in China were investigated, and the forced displacement was the main reason for the shear failure of tunnel portal linings in longitudinal and transverse directions under the geological condition of soft-hard interlayers [16]. Taking Longdongzi tunnel as a prototype, the vibration model test of tunnel portal was carried out. The results showed that the dynamic amplification effect of tunnel portal has saturation characteristics when the PGA was greater than 0.6 g [17]. The relationship between the element size of numerical calculation model and the length of seismic wave was studied by Lysmer and Kuhemeyer, and the element size of calculation model should be less than 1/10~1/8 of the minimum wavelength determined [18]. By means of numerical calculation, the seismic response laws of tunnel crossing homogeneous rock and rock-soil interface area were discussed, and the conclusion that the stratum inertial force was the leading factor of seismic damage of tunnel in the rock-soil interface area was drawn [19]. A tunnel-slope coupling numerical calculation model for tunnel portal section in upper-soft and lower-hard stratum was established, and the tunnel located in soft rock stratum bore more forced displacement than the tunnel located in hard rock stratum [20]. The relative displacement of tunnel portal linings increased obviously under the action of strong earthquake when the tunnel passed through the soft-hard interface, and the relative displacement of tunnel linings decreased with the increase of the inclination of interface [21].

All of the above studies were aimed at dynamic response of tunnel portal at interface section between the upper-soft and lower-hard stratum, which could not effectively eliminate seismic amplification effect of tunnel portal. Moreover, the above research conclusions also have certain differences. At the same time, there were relatively few projects that could be used for reference when the tunnel crosses the vertical interface section between soft and hard rock. Therefore, it is necessary to carry out shaking table model test of tunnel crossing vertical interface section between soft and hard rock in high intensity area and explore the characteristics of seismic damage and damping technology of tunnel, so as to provide theoretical reserves for the design and construction of tunnel crossing interface section of soft and hard rock in high intensity area.

2. Background

Urumqi Subway Tunnel project is located in seismic intensity area of degrees VII~VIII. The tunnel passes through the Yamak fault ($f2$), the Bagang-Petrochemical hidden fault ($f4$), the Jiujiawan fault ($f5$), and the Xishan fault ($f7$) from south to north. There are typical soil-rock interface and soft-hard rock interface in tunnel site, as shown in Figure 1. The tunnel passes through interface section of soft and hard rock, and the interface is approximately vertical. The tunnel section is horseshoe shaped with a span of 8.573 m and a height of 9.120 m. The thicknesses of primary support and secondary linings are 30 cm and 60 cm, respectively, and the buried depth is 11.8 m. The soft rock is mainly composed of strongly weathered sand gravel, while the hard rock is mainly composed of sandstone. The mechanical parameters of stratum revealed by drilling are shown in Table 1.

3. Model Experimental Design

3.1. Experimental Purpose and Grouping. On the one hand, through setting working conditions *A*, *B,* and *C*, the dynamic responses of tunnel in homogeneous stratum and interface section of soft and hard rock were compared and analyzed. And then the seismic damage characteristics of tunnel crossing interface section of soft and hard rock were explored. One the other hand, through setting working conditions *C*, *D,* and *E*, the damping effects of different absorbing joints of tunnel at interface of soft and hard rock were compared and studied. The specific grouping is shown in Table 2, and the conventional structures of absorbing joints are shown in Figures 2(a) and 2(b). The new type of absorbing joint structure of staggered absorbing joints between primary support and second lining is shown in Figure 2(c). In Figure 2, the green part represents primary support, which is composed of 30 cm thick shotcrete, and the red part represents second lining, which is composed of 60 cm thick formwork concrete.

3.2. Similar Parameter Design. According to similarity theory and research purposes, geometric similarity ratio and elastic modulus similarity ratio were selected as the basis similar parameters, and the other similarity ratios of parameters were derived based on these two parameters. Considering the size and boundary effect of model test box [22, 23], it was determined that the geometric similarity ratio of mode test was set as 30 : 1, the elastic modulus similarity ratio was set as 45 : 1, and the similarity ratios of other main physical parameters are as follows: the strain similarity ratio was set as 1 : 1, the stress similarity ratio was set as 45 : 1, and the density similarity ratio was set as 1.5 : 1.

3.3. Model Experimental Equipment and Materials. The dynamic test was performed on a three-dimensional six-degree-of-freedom seismic simulation test table, which could simulate a variety of different ground motion inputs. During the test, the seismic acceleration was applied from vibration test table surface. The test site is shown in Figure 3, and the basic parameters are shown in Table 3.

The tunnel model was built in a stiff, strong box with a length, width, and height of 2.5 m, 2.5 m, and 1.5 m, respectively, and was bolted to the steel platform of the shaking

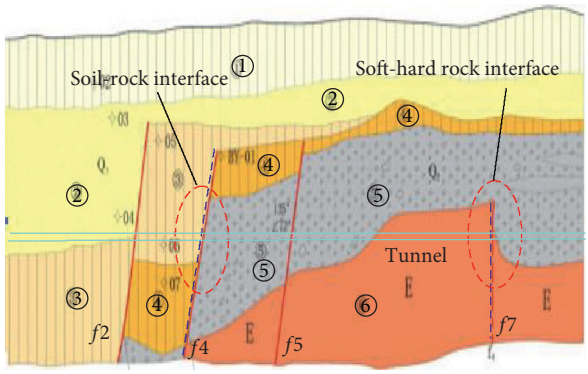

Figure 1: Geological conditions of interface section of soft and hard rock.

table. The two observation windows were set on both sides of test box, and the test box was divided into two parts: the front part and the back part, which were filled with different proportions of simulation materials to simulate the actual soft rock section and hard rock section, respectively. The test box is shown in Figure 4.

The primary support was simulated with gypsum, the second lining was simulated with steel wire and gypsum (see Figure 5), the waterproof board was simulated with polyethylene film, and the primary support and second lining were sawn into 3 mm wide gaps by saw blade according to the setting intervals to simulate the actual absorbing joints. The second lining of tunnel was C45 concrete with elastic modulus of 3.35×104 MPa, and the elastic modulus of similar materials of second lining should be 744.4 MPa according to the similar ratio of elastic modulus. Through orthogonal test, the paste-water ratio of similar materials with second lining was 1.55 : 1, and the actual measured elastic modulus was 744.8 MPa. The similar materials of surrounding rock were mixtures of barite, quartz sand, gypsum, and water. The raw material proportion was determined by orthogonal test, and the reasonable mixture ratio and physical mechanical parameters were obtained through multiple proportioning tests (see Table 4).

3.4. Seismic Loads and Boundaries

3.4.1. Seismic Load. The measured seismic waves in Wolong, Wenchuan, China, were applied to the model test. After filtering, baseline correction, and similar transformation, the time-acceleration curve of north-south direction is shown in Figure 6.

Fourier transform was carried out for the time-acceleration curve, and modal analyses of test box and tunnel-surrounding rock system were carried out. The dynamic characteristics are shown in Table 5. It can be seen from Table 5 that the predominant frequencies of test dynamic load, test box, and tunnel-surrounding rock system are not similar, so the resonance phenomenon will not occur during the model test.

3.4.2. Boundary Conditions. The polystyrene foam board with a thickness of 22.5 cm was laid on the inner wall of test box to reduce the influence of box wall on the soil in box [22, 23]. At the same time, a layer of gravel was bonded at the bottom of test box to increase the friction between bottom of box and soil in box, so as the relative sliding between bottom of box and soil in box was avoided during application of seismic loads. The boundary conditions are shown in Figure 7.

3.5. Monitoring Sections and Monitoring Points. According to the setting conditions of absorbing joints, the test monitoring sections are determined as shown in Figure 8. In each monitoring section, transverse strain gauge H (symmetrically arranged inside and outside of lining), longitudinal strain gauge L (symmetrically arranged inside and outside of lining), and acceleration sensor S were arranged on vault, side wall, and invert of tunnel monitoring section. At the same time, dial gauge Q was also arranged on vault of tunnel monitoring section. The layout of specific monitoring points is shown in Figure 8(c).

4. Characteristics of Seismic Damage of Tunnel Crossing Interface of Soft and Hard Rock

4.1. Comparative Analysis of Peak Acceleration of Ground. In order to facilitate comparative analysis, the peak ground acceleration (PGA) measured at monitoring point of working condition A is taken as the reference point. The PGA amplification factor is named as the ratio of measured PGA in vertical direction of side wall and PGA in horizontal direction of vault under working condition B and working condition C to the corresponding point of working condition A. The PGA amplification factors under different working conditions are listed in Table 6.

It can be seen from Table 6 that the PGA amplification factors in homogeneous soft rock (working condition A) are greater than those in homogeneous hard rock (working condition B). The average PGA amplification factor of vertical direction of side wall in homogeneous soft rock is increased by 83.40%, and the average amplification factor of horizontal direction of vault in homogeneous soft rock is increased by 66.40%. The above analysis shows that, under the same inertia force of stratum, the damage degree of tunnel linings under homogeneous soft rock is much greater than that under homogeneous hard rock.

Under the geological condition of interface between soft and hard rock (working condition C), the average PGA amplification factor of vertical direction of side wall in soft rock section is increased by 66.33%, and the average PGA amplification factor of horizontal direction of vault in soft rock section is increased by 43.33%. But the influence of stratum inertial force on side wall and vault of tunnel lining of soft rock section under working condition C is 17.07% and 23.07% lower than that under working condition B, and the influence of stratum inertial force on tunnel lining of hard rock section under working condition C is slight. It shows that stratum inertial force mainly affects the soft rock

Table 1: Mechanical parameters of stratum.

Property of rock	Density (g·cm^{-3})	Cohesion (kPa)	Friction angle (°)	Modulus of elasticity (MPa)	Poisson's ratio
Gravel	1.85 ~ 2.05	87 ~ 126	19.8 ~ 30.5	212 ~ 438	0.24 ~ 0.33
Sandstone	1.98 ~ 2.26	205 ~ 267	25.7 ~ 37.8	2 886 ~ 6 484	0.19 ~ 0.21

Table 2: Experimental working conditions.

Working conditions	Experiment contents
A	Homogeneous formation (hard rock), no absorbing joint
B	Homogeneous formation (soft rock), no absorbing joint
C	Interface of soft and hard rock, no absorbing joint
D	Interface of soft and hard rock, only setting absorbing joint for second lining
E	Interface of soft and hard rock, staggered absorbing joints of primary support and second lining (absorbing joint of second lining is set according to the optimal absorbing joint interval, the interval of primary support absorbing joint is 3 m, 6 m, 9 m and 12 m respectively)

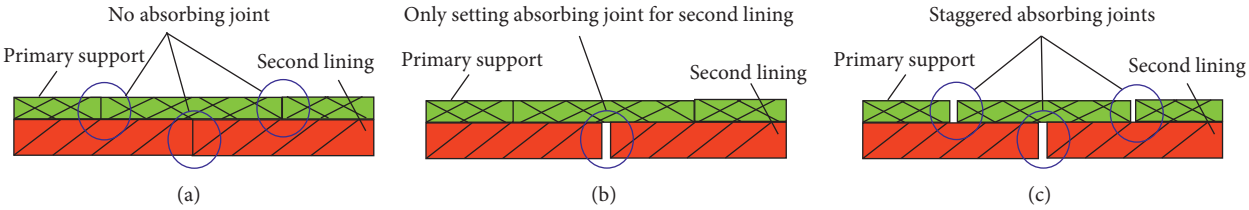

Figure 2: Setting of different absorbing joints. (a) Working condition *C*. (b) Working condition *D*. (c) Working condition *E*.

Figure 3: Field of test.

Table 3: Parameters of vibration table.

Shaking table size (m ∗ m)	Maximum capacity of load (t)	Frequency range (Hz)	Maximum displacement (mm)		Maximal acceleration of full-load condition (g)		Maximal acceleration of no-load condition (g)	
			Horizontal	Vertical	Horizontal	Vertical	Horizontal	Vertical
6 × 6	60	0.1 ~ 100	±150	±150	1	0.8	3.5	3

section under the geological condition of interface between soft and hard rock, but hardly affects the hard rock section.

4.2. Displacement Difference of Interface. The vertical displacements of vaults in each monitoring section are extracted, and vault displacement increments under working conditions *A* (homogeneous hard rock), *B* (homogeneous soft rock), and *C* (interface of soft and hard rock) relative to working condition *A* are plotted in Figure 9.

It can be seen from Figure 9 that, under the action of stratum inertia force, the displacement curves of vaults of each monitoring section measured under working condition

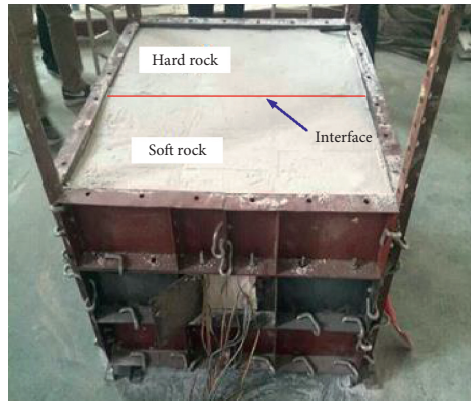

Figure 4: Test box of seismic simulation.

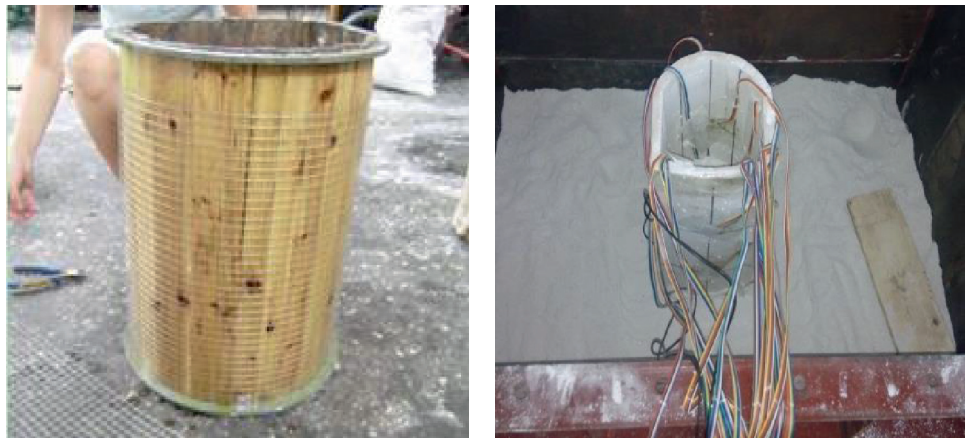

(a) (b)

Figure 5: Model of second lining. (a) Steel wire. (b) The gypsum of second lining.

Table 4: Test results and mixture ratio of similar materials of surrounding rock.

Lithology	Mixture ratio of materials (%)				Test results		
	Barite	Quartz sand	Gypsum	Water	Cohesion (kPa)	Friction angle (°)	Modulus of elasticity (MPa)
Soft rock	40	123	2.2	15	2.2	29.8	8
Hard rock	60	113	3.5	10	5.0	33.4	90

The prototype of soft rock is gravel layer, while the prototype of hard rock is sandstone.

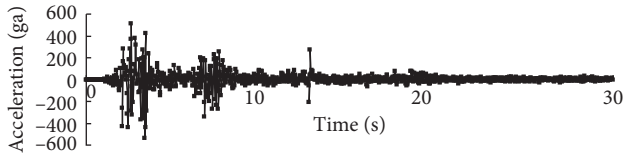

Figure 6: Curve of time-acceleration of south-north direction.

A and working condition B are basically straight lines; that is, there are no obvious displacement differences along the longitudinal direction of tunnel under working condition A and working condition B. Under the geological condition of interface between soft and hard rock (working condition C), the vault displacement values in hard rock section are similar, but the vault displacement values of each monitoring section in soft rock section near interface increase obviously; that is, there is a significant displacement difference at the interface of soft and hard rock.

The authors believe that a large number of circular staggered platform cracks (Figure 10) occurring in tunnel lining at interface of soft and hard rock in literatures [7–9] are related to the displacement difference at the interface between soft and hard rock. The explanation is as follows: the tunnel can be regarded as a cantilever beam buried in hard rock, and the free end is constrained by the stratum of soft rock section, so the displacement of root of cantilever beam (located in hard rock section) is small. While the lining in

Table 5: Dynamic characteristics.

Predominant frequency (Hz)				
Curve of time-acceleration			Test box	System of tunnel-surrounding rock
East-west	North-south	Vertical		
16	17	21	42.81	7.32

(a) (b)

Figure 7: Conditions of boundary. (a) Polystyrene foam board of side wall. (b) Gravel of bottom.

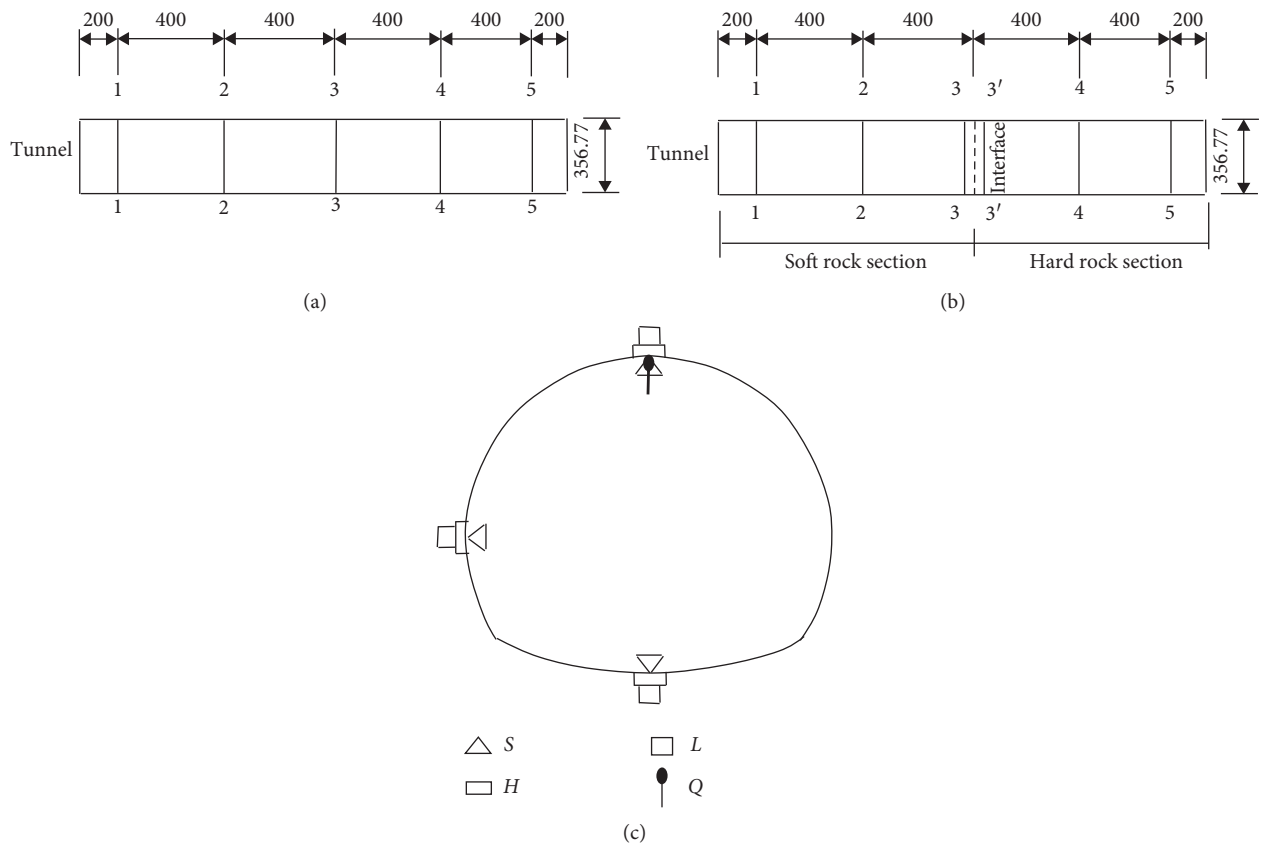

Figure 8: Layout of monitoring sections and points (unit: mm). (a) Monitoring sections of homogeneous soft rock or hard rock. (b) Monitoring sections of interface of soft and hard rock. (c) Monitoring points.

Table 6: Amplification factors of PGA.

Section	Direction	PGA amplification factor		
		Working condition *A*	Working condition *B*	Working condition *C*
1–1	Vertical	1.00	1.85 (85%)	1.67 (67%)
	Horizontal	1.00	1.68 (68%)	1.43 (43%)
2–2	Vertical	1.00	1.84 (84%)	1.66 (66%)
	Horizontal	1.00	1.66 (66%)	1.42 (42%)
3–3	Vertical	1.00	1.82 (82%)	1.66 (66%)
	Horizontal	1.00	1.66 (66%)	1.42 (42%)
4–4	Vertical	1.00	1.84 (84%)	1.12 (12%)
	Horizontal	1.00	1.66 (66%)	1.07 (7%)
5–5	Vertical	1.00	1.82 (82%)	1.06 (6%)
	Horizontal	1.00	1.66 (66%)	1.03 (3%)

The values in brackets are the percentage increase of PGA amplification factor under condition of soft rock or interface of soft and hard rock relative to condition of hard rock.

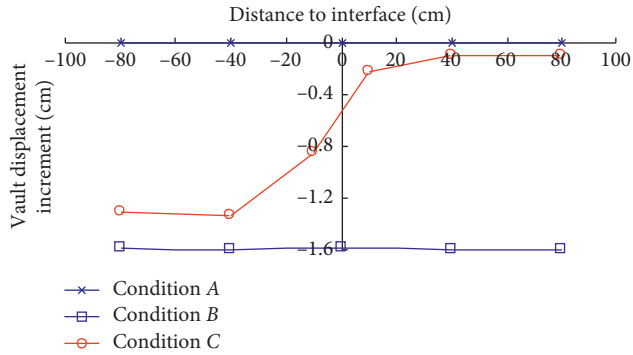

Figure 9: Forced displacement of vault at different monitoring sections.

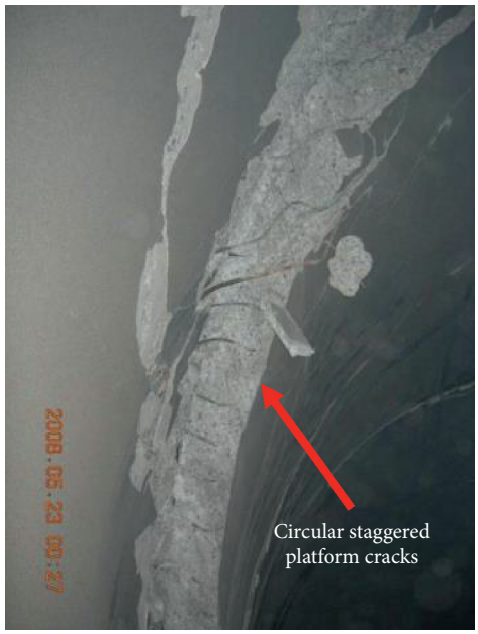

Figure 10: Circular staggered platform cracks after earthquake.

soft rock section shows obvious "swings" due to action of stratum inertial force, there is a large displacement difference between the two sides of interface of soft and hard rock, which causes the lining to show circumferential staggered platform cracks. Obviously, the higher the seismic intensity is, the more obvious the above phenomenon is.

Based on the analysis in this section, it can be seen that, under the geological condition of soft rock, the seismic damage of tunnel is mainly affected by inertial force of stratum. Under the geological condition of interface between soft rock and hard rock, the seismic damage of tunnel is mainly caused by forced displacement (displacement difference between the two sides of interface of soft rock and hard rock), followed by inertial force of stratum.

4.3. Effect of Absorbing Joint at Interface of Soft and Hard Rock. At present, absorbing joints and shock absorption layers are commonly used in tunnel as damping measures. The cost and construction difficulty of setting shock absorption layers are relatively large, and absorbing joints can be set in combination with construction joints, which makes the cost low and the construction difficulty small [24]. In order to deal with the circular staggered platform cracks caused by displacement difference at the interface of soft and hard rock, conventional type of absorbing joint (only setting absorbing joint for second lining) and new type of absorbing join (staggered absorbing joints of primary support and second lining) should be set. In this section, the effects of different setting lengths and different setting types of absorbing joints are discussed under geological condition of interface of soft and hard rock.

4.4. Reasonable Length of Absorbing Joint. Taking the working condition *D* (interface of soft and hard rock, only setting absorbing joint of second lining) as a prototype, the reasonable setting lengths of absorbing joints at interface between soft and hard rock are studied by changing the setting intervals of absorbing joints. Six cases of no absorbing joint and absorbing joints with intervals of 3 m, 6 m, 9 m, 12 m, and 15 m are studied.

4.4.1. Analysis of Principal Tensile Stress. The tunnel lining is composed of reinforced concrete. Under the action of seismic load, it is easy to produce large local tensile stress and

promote the lining cracking. Therefore, according to formula (1), the principal tensile stresses are calculated by extracting the strains at the monitoring points of vault, side wall, and invert of each monitoring section in six cases, as shown in Figure 11.

$$\begin{matrix}\sigma_1\\ \sigma_3\end{matrix} = \frac{E}{1-\nu^2}\left[\frac{1+\nu}{2}(\varepsilon_0+\varepsilon_{90}) \pm \frac{1+\nu}{\sqrt{2}}\sqrt{(\varepsilon_0-\varepsilon_{45})^2+(\varepsilon_{45}-\varepsilon_{90})^2}\right], \tag{1}$$

where σ_1 is the first principal stress of lining, σ_3 is the third principal stress of lining, $E$is the elastic modulus of lining, $\nu$is Poisson's ratio of lining, and ε_0, $\varepsilon_{45}$and ε_{90} are the strains in 0°, 45°, and 90° directions of observation point of lining.

It can be seen from Figure 10 that the distribution laws of principal tensile stresses of vault, side wall, and invert of tunnel are similar. The maximum principal tensile stress is at the interface of soft and hard rock, and it shows a normal distribution law of weakening to both sides. The reduction percentage of principal stress at the same position after setting absorbing joint compared with that before setting absorbing joint is defined as the damping ratio. The setting of absorbing joint has a significant damping effect on tunnel at interface section of soft and hard rock. Under the conditions of 3 m, 6 m, 9 m, 12 m, and 15 m intervals of absorbing joints, the minimum principal tensile stress damping ratios of vault, side wall, and invert of tunnel at interface of soft and hard rock are 72.09%, 62.66%, and 47.47%, respectively, and the maximum principal tensile stress damping ratios are 86.16%, 84.39%, and 76.71%, respectively.

In order to further clearly show the damping effect of absorbing joints with different intervals, the maximum principal tensile stresses at interface of soft and hard rock under different intervals of absorbing joints are plotted in Figure 12.

It can be seen from Figure 11 that the maximum principal tensile stress also tends to increase with the increase of interval of absorbing joint. When the interval of absorbing joint increases from 3 m to 9 m, the maximum principal tensile stress increases approximately linearly. When the interval of absorbing joint increases from 9 m to 15 m, the increasing trend of maximum principal tensile stress slows down. The small lining formwork trolley is convenient to set small absorbing joint interval in high intensity area, which can significantly improve the damping effect of tunnel lining. However, most of the actual lining formwork trolleys are 9 m, 12 m, and 15 m, so it is not necessary to be too tangled when determining the interval parameters of absorbing joints. According to the length of actual lining formwork trolley, the damping effect of absorbing joint with corresponding interval is equivalent. The damping ratio of principal tensile stress is above 47.5%, and the damping effect is significant.

4.4.2. Analysis of Internal Force and Safety Factor. The bending moment and axial force of tunnel lining are obtained by the following formulas:

$$\begin{aligned} N &= \frac{1}{2}E(\varepsilon_{\text{in}}+\varepsilon_{\text{out}})bh,\\ M &= \frac{1}{12}E(\varepsilon_{\text{in}}-\varepsilon_{\text{out}})bh^2, \end{aligned} \tag{2}$$

where b is the longitudinal unit length of lining, h is the thickness of lining, E is the elastic modulus of lining, and ε_{in} and ε_{out} are the strains measured by inner and outer strain gauges of lining, respectively.

The safety factor of tunnel lining is obtained by the following formulas:

$$\begin{aligned} KN &\le \phi\alpha R_\alpha b_1 h_1,\\ KN &\le \phi\frac{1.75R_1 b_1 h_1}{6e_0/h-1}, \end{aligned} \tag{3}$$

where R_α is the ultimate compressive strength of concrete, R_1 is the ultimate tensile strength of concrete, K is the safety factor, N is the axial force, b_1 is the width of section, h_1 is the thickness of section, ϕ is the longitudinal bending coefficient, and α is the eccentric influence coefficient of axial force.

The bending moment and axial force at vault of each monitoring section are plotted in Figure 13. It can be seen from Figure 12 that, after setting absorbing joints of 3 m, 6 m, 9 m, 12 m, and 15 m, the bending moments of vault at interface of soft and hard rock are reduced by 69.54%, 65.52%, 51.29%, 43.06%, and 40.74%, respectively, and the axial forces of vault are reduced by 88.88%, 84.34%, 81.31%, 75.76%, and 72.72%, respectively. The damping effect of setting absorbing joint on internal force of tunnel lining at interface of soft and hard rock is significant. The damping rate of bending moment is more than 40.7%, and the damping rate of axial force is more than 72.7%. Moreover, the setting of absorbing joint can make axial force of lining at interface of soft and hard rock tend to be uniform. Whether or not the absorbing joint is set, the internal force of tunnel lining in soft rock section is obviously greater than that in hard rock section, and the soft rock side of interface section between soft and hard rock should be paid more attention in design and construction of seismic resistance and absorption in actual high intensity area.

The distribution of safety factor of tunnel vault at each monitoring section is shown in Figure 14, and the relationship between safety factor of vault and interval of absorbing joint at interface section between soft and hard rock is shown in Figure 15.

It can be seen from Figures 14 and 15 that the safety factor of hard rock section is much greater than that of soft rock section. With the increase of interval of absorbing joint, the safety factor of tunnel lining tends to decrease. When the interval of absorbing joint increases from 3 m to 9 m, the safety factor of tunnel lining tends to decrease approximately linearly, and when the interval of absorbing joint increases from 9 m to 15 m, the decreasing trend of safety factor of tunnel lining tends to be gentle. The above analysis also shows that the actual lining formwork trolley is mostly 9 m, 12 m, and 15 m, and the effect of absorbing joint with corresponding interval reserved according to the length of

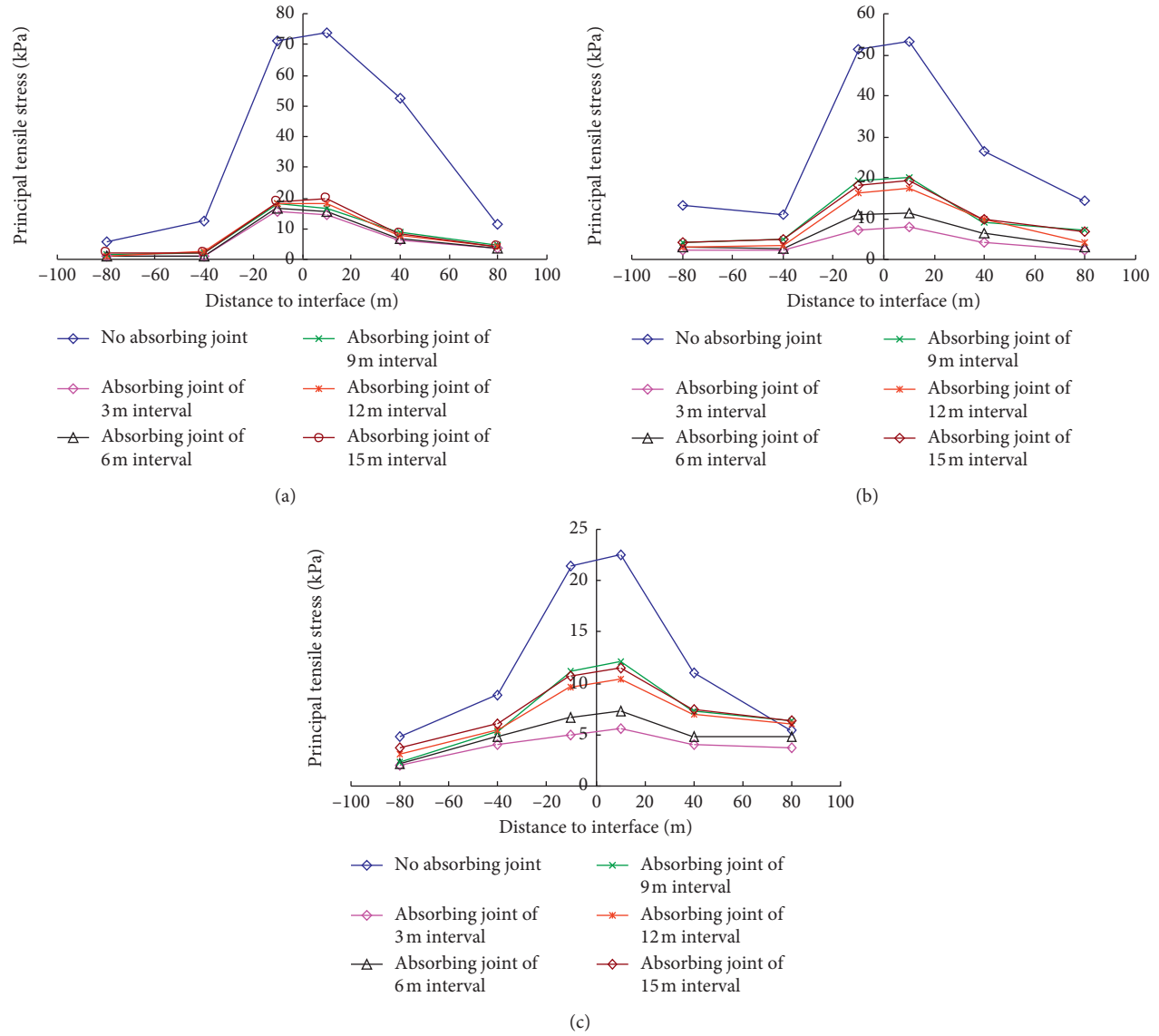

Figure 11: Principal tensile stresses of different parts of each monitoring section. (a) Vault of tunnel. (b) Side wall of tunnel. (c) Invert of tunnel.

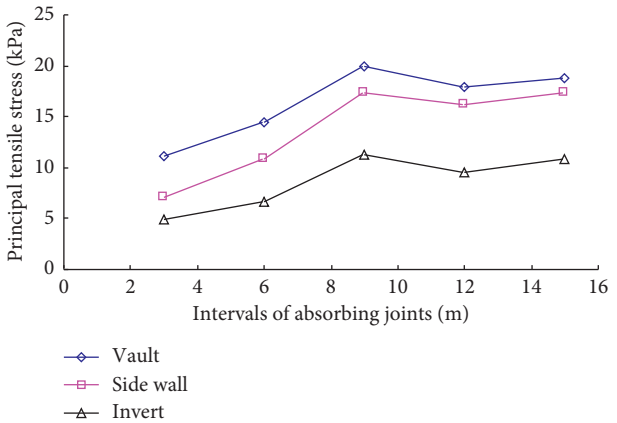

Figure 12: Relationship between principal tensile stress and interval of absorbing joint.

lining formwork trolley is equivalent, which provides a certain theoretical basis for the design and construction of absorbing joint in actual tunnel engineering.

4.5. Reasonable Type of Absorbing Joint. In actual tunnel engineering, the second lining absorbing joint is generally set synchronously according to the length of lining formwork trolley and waterproof requirements; that is, the second lining absorbing joint and the construction joint are set in the same section. According to the length of commonly used lining formwork trolley, only absorbing joint with 12 m interval set for second lining is studied in this section. A new type of absorbing joint is proposed, which is the structure of staggered absorbing joints between primary support and second lining (see Figure 2). The setting interval of second lining absorbing joint is also 12 m, and the

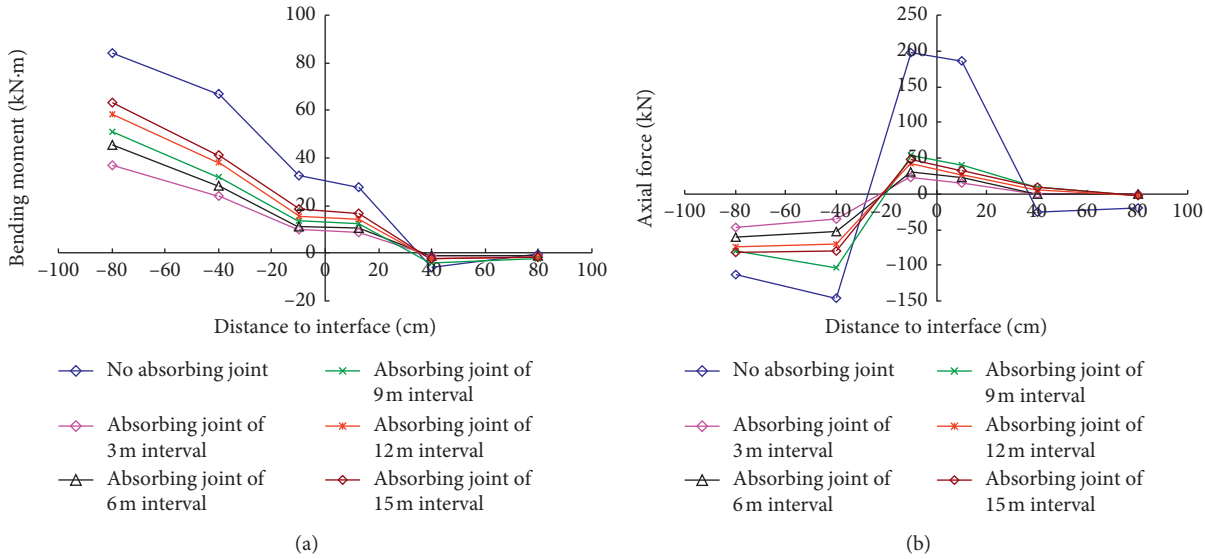

Figure 13: Internal force of tunnel vault at each monitoring section. (a) Bending moment of vault. (b) Axial force of vault.

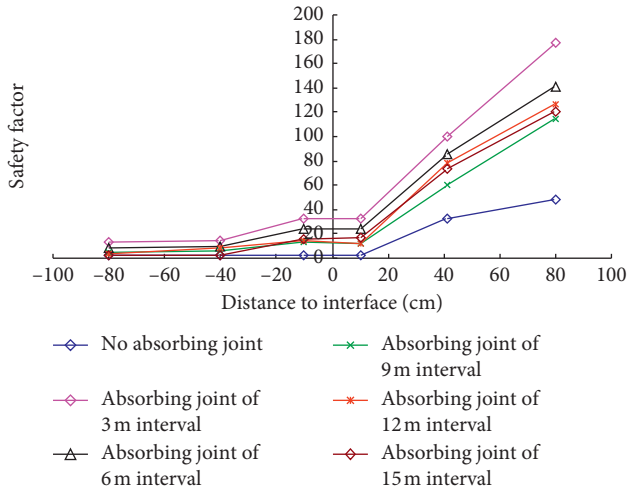

Figure 14: Safety factor of tunnel vault at each monitoring section.

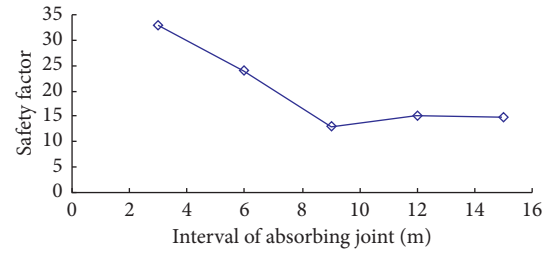

Figure 15: Relationship between safety factor of vault and interval of absorbing joint.

intervals of primary support absorbing joint are set at 3 m, 6 m, 9 m, and 12 m for comparative analysis. The comparison results of principal tensile stress, bending moment, and axial force with different setting types under the geological section of interface between soft and hard rock are plotted in Figure 16.

It can be seen from Figure 16 that, compared with the measure of only setting second lining absorbing joint, the principal tensile stresses of vault are reduced by 19.94%, 15.85%, 8.74%, and 3.83%, the bending moments are reduced by 19.07%, 14.44%, 11.03%, and 4.31%, and the axial forces are reduced by 19.04%, 16.66%, 13.09%, and 7.14%, respectively, by setting new absorbing joints with different intervals of 3 m, 6 m, 9 m, and 12 m at interface section of soft and hard rock.

It shows that the new type of absorbing joint can further enhance damping capacity of tunnel lining at interface between soft and hard rock. The damping effect of stress and internal force of lining is increased by nearly 20% when 3 m interval of absorbing joint is set in primary support and 12 m interval of absorbing joint is set in second lining. The main reason that a new type of absorbing joint can further improve damping capacity of tunnel lining at interface between soft and hard rock is that the setting of absorbing joint in primary support makes distribution of surrounding rock pressure at interface section between soft and hard rock more uniform, and the local stress concentration is relieved to a certain extent.

5. Suggestions on Setting of Absorbing Joint in Practical Engineering

5.1. Suggestions on Setting of Absorbing Joint in Primary Support. In order to enhance the antibreaking capacity of primary support, the rubber shotcrete can be applied within the width of absorbing joint (rubber shotcrete is ordinary

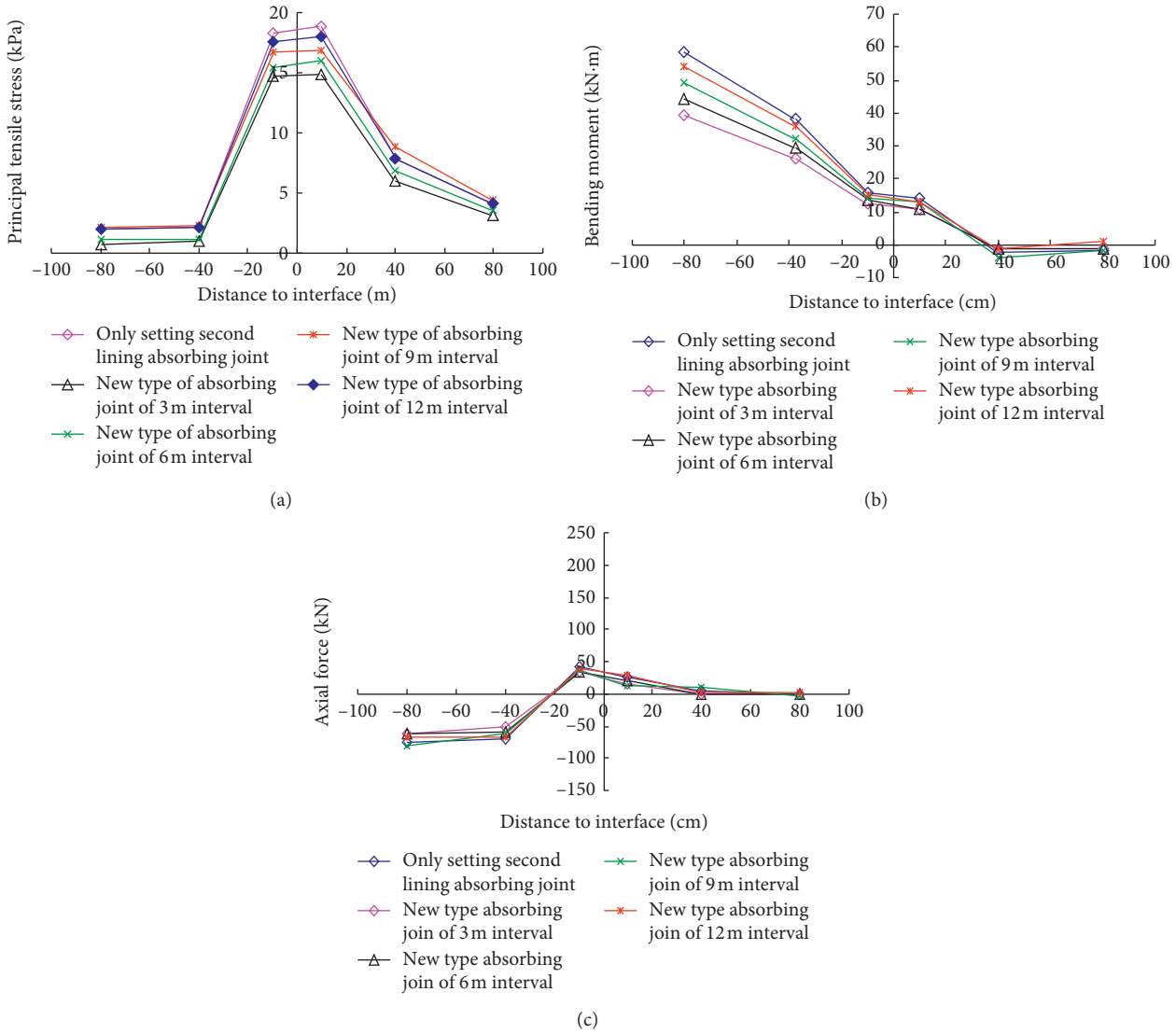

Figure 16: Internal force of tunnel vault at each monitoring section. (a) Principal tensile stress of vault. (b) Bending moment of vault. (c) Axial force of vault.

shotcrete with rubber particles added to improve the toughness of shotcrete). The thickness of rubber shotcrete at absorbing joint is 1/2 of original design thickness of primary support. The rubber shotcrete is also used to replace ordinary shotcrete within 3~5 times of the width (▽) of absorbing joint on both sides of absorbing joint, and the rubber shotcrete thickness at absorbing joint gradually increases to the design thickness of primary support, so as to realize the flexible hinge connection and stiffness gradual change at absorbing joint in primary support and improve antibreaking ability. The structural sketch of absorbing joint in primary support is shown in Figure 17.

5.2. Suggestions on Setting of Absorbing Joint in Second Lining. The setting of second lining absorbing joint can be combined with the length of lining formwork trolley and the waterproof requirements; that is, the second lining absorbing joint and the construction joint are set on the same section. The construction joint itself needs to be equipped with a medium buried rubber waterstop and a back stick waterstop on water face to achieve the purpose of waterproofing. The rubber waterstop itself can be used as a part of damping material for second lining absorbing joint to block longitudinal transmission of seismic waves. At the same time, the asphalt sand mixture is used to fill the inner of absorbing joint, and the caulking paste is used to block the back water surface of absorbing joint to further enhance damping effect. The structural sketch of absorbing joint in second lining is shown in Figure 18.

The above technical scheme can effectively weaken and block the path of seismic waves along the longitudinal propagation of tunnel, and the antibreaking ability of tunnel can be significantly improved.

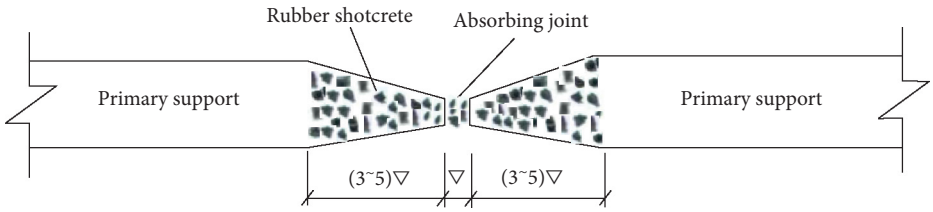

Figure 17: Structural sketch of absorbing joint in primary support.

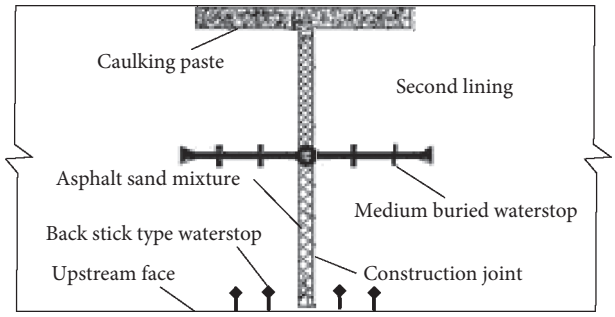

Figure 18: Structural sketch of absorbing joint in second lining.

6. Conclusions

(1) The seismic damage of tunnel is mainly affected by stratum inertial force under soft rock geological conditions, while the seismic damage of tunnel is mainly caused by forced displacement, followed by stratum inertial force under the geological conditions of interface section between soft and hard rock.

(2) The setting of absorbing joint can effectively improve the aseismic capacity of tunnel at interface section between soft and hard rock. The damping ratio of principal tensile stress of tunnel lining is more than 47.5%, and the damping ratio of internal force of tunnel lining is more than 40.7%.

(3) The damping effect of new type of absorbing joint structure is better than that of the common structure with absorbing joint only in second lining. The maximum damping effect of tunnel is increased by nearly 20%. It is recommended to adopt the new type of absorbing joint structure when the tunnel passes through the interface section between soft and hard rock in high intensity area.

(4) In the actual construction process of tunnel engineering, the new type of absorbing joint structure is proposed as follows: the setting interval of second lining absorbing joint is the same as the length of lining formwork trolley, and the interval of primary support absorbing joint can be set according to the length of excavation footage. The filling material in second lining absorbing joint can be shared with the rubber waterstop set in construction joint, and the primary support absorbing joint can be realized by injecting mixture of rubber particles and shotcrete.

Data Availability

The data used to support the findings of this study are included within the article.

Conflicts of Interest

The authors declare that there are no conflicts of interest regarding the publication of this paper.

Acknowledgments

The authors appreciate the support from the National Natural Science Foundation of China (no. 51478277) and the Hebei Province Key Research and Development Project of China (no. 172776471).

References

[1] Y. Shen, B. Gao, and Y. Wang, "Structural dynamic properties analysis for portal part of mountain tunnel in strong earthquake area," *Chinese Journal of Rock Mechanics and Engineering*, vol. 28, no. 1, 2009.

[2] M. Kiani, T. Akhlaghi, and A. Ghalandarzadeh, "Experimental modeling of segmental shallow tunnels in alluvial affected by normal faults," *Tunnelling and Underground Space Technology*, vol. 51, pp. 108–119, 2016.

[3] L. I. Lin, C. He, P. Geng et al., "Study of shaking table model test for seismic response of portal section of shallow unsymmetrical loading tunnel," *Chinese Journal of Rock Mechanics and Engineering*, vol. 30, no. 12, 2011.

[4] C. Xin, B. Gao, and J. Zhou, "Shaking table tests on performances of anti-seismic and damping measures for fault-crossing tunnel structures," *Chinese Journal of Geotechnical Engineering*, vol. 36, no. 8, 2014.

[5] D. Y. Wang, S. Q. Jia, G. Y. Cui et al., "Model test on bearing characteristics of basalt fiber-reinforced concrete lining," *Advances in Materials Science and Engineering*, vol. 2020, Article ID 3891343, 10 pages, 2020.

[6] P. Geng, Y. He, C. He et al., "Study of shaking table model test for seismic response of portal section of shallow unsymmetrical loading tunnel," *Chinese Journal of Rock Mechanics and Engineering*, vol. 33, no. 2, pp. 358–365, 2014.

[7] B. Gao, Z. Wang, S. Yuan et al., "Lessons learnt from damage of highway tunnels in Wenchuan earthquake," *Journal of Southwest Jiaotong University*, vol. 44, no. 3, pp. 336–374, 2009.

[8] G. Y. Cui and X. L. Wang, "Model test study on the anti-breaking technology of reducing dislocation layer for subway interval tunnel of the stick-slip fracture," *Advances in Civil Engineering*, vol. 2019, Article ID 4328103, 9 pages, 2019.

[9] Z. Z. Wang, Y. J. Jiang, and C. A. Zhu, "Seismic energy response and damage evolution of tunnel lining structures,"

European Journal of Environmental and Civil Engineering, vol. 19, 2019.

[10] D. Y. Li, Z. Y. Han, X. L. Sun et al., "Dynamic mechanical properties and fracturing behavior of marble specimens containing single and double flaws in shpb tests," *Rock Mechanics and Rock Engineering*, vol. 52, 2019.

[11] H. Chen, X. Li, W. Yan, S. Chen, and X. Zhang, "Shaking table test of immersed tunnel considering the geological condition," *Engineering Geology*, vol. 227, pp. 93–107, 2017.

[12] Z. Chen, W. Chen, Y. Li, and Y. Yuan, "Shaking table test of a multi-story subway station under pulse-like ground motions," *Soil Dynamics and Earthquake Engineering*, vol. 82, pp. 111–122, 2016.

[13] M. R. Moghadam and M. H. Baziar, "Seismic ground motion amplification pattern induced by a subway tunnel Shaking table testing and numerical simulation," *Soil Dynamics and Earthquake Engineering*, vol. 83, pp. 81–97, 2016.

[14] Z. Bao, Y. Yuan, H. Yu et al., "Multi-scale physical model of shield tunnels applied in shaking table test," *Soil Dynamics and Earthquake Engineering*, vol. 100, pp. 465–479, 2017.

[15] H. Xu, T. Li, L. Xia, J. X. Zhao, and D. Wang, "Shaking table tests on seismic measures of a model mountain tunnel," *Tunnelling and Underground Space Technology*, vol. 60, pp. 197–209, 2016.

[16] Z. Z. Wang, Y.-J. Jiang, C. A. Zhu, and T. C. Sun, "Shaking table tests of tunnel linings in progressive states of damage," *Tunnelling and Underground Space Technology*, vol. 50, pp. 109–117, 2015.

[17] D. Wu, B. Gao, Y. Shen et al., "Shaking table test study of seismic dynamic response of tunnel entrance slope," *Rock and Soil Mechanics*, vol. 35, no. 7, 2014.

[18] J. Lysmer and R. L. Kuhlemeyer, "Finite dynamic model for infinite media," *Journal of Engineering Mechanics*, vol. 95, no. 4, pp. 859–877, 1969.

[19] Y. Yin and T. Li, "Analysis and study of the seismic failure mechanism and aseismic measures of a tunnel structure in the rock-soil interface area," *Modern Tunnelling Technology*, vol. 50, no. 4, pp. 84–91, 2013.

[20] G. Cui, M. Wang, Y. U. Li et al., "Analysis of seismic damage and mechanism of portal structure of highway tunnel in Wenchuan earthquake," *Chinese Journal of Geotechnical Engineering*, vol. 35, no. 6, 2013.

[21] Y. Shen, C. Zou, Z. Jin et al., "A study of the dynamic response characteristics of a tunnel structure through an interface of soft and hard rock," *Modern Tunnelling Technology*, vol. 52, no. 3, pp. 95–101, 2015.

[22] S. Hou, L. Tao, X. Zhao et al., "Shaking table test for dynamic respinse in portal section of mountain tunnel based on different vibration directions," *Journal of Central South University: Science and Technology*, vol. 47, no. 3, pp. 994–1001, 2016.

[23] S. Jiang, D. Wen, and S. Zheng, "Largescale shaking table test for seismic response in portal section of Galongla tunnel," *Chinese Journal of Rock Mechanics and Engineering*, vol. 30, no. 4, pp. 649–656, 2011.

[24] D. Wang, G. Cui, and J. Yuan, "Model experimental study on effect of reducing dislocation measures undering stick-slip fault dislocation of tunnel," *Chinese Journal of Geotechnical Engineering*, vol. 40, no. 8, pp. 1515–1521, 2018.